Nonlinear and curvature effects on peristaltic flow of (Cu–Al_2O_3) Hybrid Nanofluid in a Channel with Heat Transfer

Submitted by

Mostafa Goda Keshta

Arab East College, Riyadh, Saudi Arabia.

DOI:

https://doi.org/10.21608/ijaefs.2025.419841

IJAEFS

International Journal of Administrative, Economic and Financial Sciences

Volume (4), Issue (12), January 2025

E-ISSN: 2812-6408 **P-ISSN: 2812-6394**

https://ijaefs.journals.ekb.eg/

Publisher

Association of Scientific Research Technology and the Arts

https://srtaeg.org/

Nonlinear and curvature effects on peristaltic flow of (Cu–Al_2O_3) Hybrid Nanofluid in a Channel with Heat Transfer

Submitted by

Mostafa Goda Keshta

Arab East College, Riyadh, Saudi Arabia.

ABSTRACT

In this investigation, the flow of an incompressible viscous fluid driven by the travelling waves along the boundaries of a symmetric channel is studied when inertia and streamline curvature effects are not negligible, where the flow of Al_2O_3 / blood nanofluid and (Cu–Al_2O_3) / blood hybrid Nano fluid has been employed to investigate the behaviour of flow and heat transfer.

An asymptotic solution is obtained to second order in the wave number, a ratio of channel width to the wavelength, giving the curvature effects. A domain transformation is used to transform the channel of variable cross section to a uniform cross section, and this facilitates in easy way of finding closed form solutions at higher orders. The relation connecting the pressure gradient and time rate of flux is obtained. The analysis also includes three different shapes of copper Nano-composites, namely, platelet, cylinder and brick- shaped. The impact of various embedded parameters on the flow and heat transfer distributions have been demonstrated through the graphs. All the flow properties, temperature profile and rate of heat transfer at the walls are greatly

influenced by the presence of copper nanoparticles. Furthermore, it was observed that the platelet shaped Nano-composites provide a better heat transfer ability as compared to the other shapes of Nano-particles. The effects of inertia and curvature on pumping, trapping and shear stress are discussed for symmetric channels and compared with the existing results in the literature.

KEYWORDS: **(Cu–Al_2O_3)** / blood hybrid Nano fluid; heat transfer; inertia; curvature; peristaltic flow.

1 Introduction: -

Hybrid Nano-fluids have an active role in a large area of the applications of heat transfer like the heating of solar, cooling in buildings, heating in buildings, nuclear cooling, generators cooling, electric cooling, refrigeration, lubrications, thermal storage, welding and automobile radiators. Also play an active role in the industry, where exist a lot of the applications and features such high thermal efficiency and chemical stability. In these applications the hybrid nano fluids depend on these features can perform efficiently if we compare it with nanofluids. Hybrid Nano-fluids are made by dispersing two or more variant kinds of nanoparticles in base fluid or composite tiny structure in a base fluid .In addition to it result development the pressure drop and heat transfer features through exchange between minuses and pluses of unique suspension .it is reported that about only 5% of (Cu–Al_2O_3) nanoparticles refer to rising the average of Nusselt number $\overline{Nu}$ to 5.4 from 4.9 but if we add 5% of (Al_2O_3) nanoparticles will find the average of Nusselt number $\overline{Nu}$ rise 4.9 to 5.36.So we can say that Hybrid Nano-fluids are an advanced kind of nanofluids which show a noticeable thermal efficiency compared with nanofluids. There are a lot of studies in this field introduce

different models which demonstrate the effects of nanocomposite shapes such as the platelet- shaped, cylinder- shaped and brick- shaped. In the other hand when we choose the materials of the particles which can improve the positive advantages of each other and hide the disadvantages of just one material for example Al_2O_3 is lower thermal conductivity as compared to the metallic nanoparticles such as zinc, Aluminium, copper etc, which include great thermal conductivity. It is necessary to say that the addition of metallic tiny particles like copper (Cu) into a nanofluid based on Al_2O_3 nanoparticles can improve the properties of thermo physical of the blend.

in this paper we consider (Cu–Al_2O_3) / blood hybrid Nano fluid flow driven by the travelling sinusoidal waves along the upper and lower walls of a symmetric channel when streamline curvature and inertia effects are in our accounts. The solution is obtained up to second order in δ which is the ratio between channel width and wavelength .in order to find complete closed form solutions at higher orders we choose a transformation to transform the channel of variable cross section to a uniform cross section (the domain of the variable cross section channel into a channel with straight walls). The effects of streamline curvature and inertia on trapping, shear stress and pumping are discussed with hybrid nano-fluids.

Peristaltic pumping is the mechanism of transport of fluid by a wave of expansion or contraction from lower pressure to higher pressure regions. In general, we can prescribe peristalsis, the process of pumping fluids in a tube or channel and represent it here by an infinite train of progressive sinusoidal waves in the walls of a two dimensional of a symmetric channel with respect to the centreline. we have two approaches to deal with the problems of peristaltic pumping, the first in the laboratory (fixed) frame and other in wave(moving) frame. By following these methods, many specialists in engineering

and applied mathematics have studied the mechanical aspects of fluids in flows. Since the presence of moving boundaries and nonlinearities we find that the analytical solution for the general problem is not easy so, it is necessary to find general simplifying assumptions in addition to fluid flow parameters and geometrical parameters.

2 The mathematical description

Contemplate peristaltic transport of a viscous incompressible Newtonian blood - based (Cu-Al_2O_3) hybrid nano fluid flow in a symmetric channel with supple walls. The channel is generated by sinusoidal waves on the channel walls travelling with speed c and amplitude a .The lower and upper walls of the channel are maintained at the different temperatures T_l and T_u .

Consider the Cartesian coordinate system in the fixed frame $(\bar{x}, \bar{y})$, the diagram of the symmetric channel is given by (Fig.1)

$$\bar{y}(\bar{x}, \bar{t}) = \bar{\eta} = d + s(\bar{x} - c\bar{t}) , \qquad T = T_u \qquad \text{Upper wall}$$

$$\bar{y}(\bar{x}, \bar{t}) = -\bar{\eta} = -d - s(\bar{x} - c\bar{t}) , \qquad T = T_l \qquad \text{Lower wall} \qquad (2.1)$$

Where s is an arbitrary periodic function, $\bar{t}$ is the time and d is the half mean width of the symmetric channel. In order to study the motion in wave frame, we Consider the Cartesian coordinate system in the wave frame (x, y).

If we assume that the pressure difference Δp across the channel is constant [3] and the length of the channel L is an integral multiple of the wavelength λ ,the motion in wave frame remains steady and the velocity of the waves on the walls is the same C .In order to convert from the fixed frame to the wave frame ,we have the transformation

$\bar{x} - c\bar{t} = x, \bar{y} = y$, $\bar{u} - c = u$, $\bar{v} = v$, and $\bar{p}(\bar{x}, \bar{y}, \bar{t}) = p(x, y)$ (2.2)

Where $(\bar{u}, \bar{v})$ and (u, v) are the velocity components, $\bar{p}$ and p are the pressure in the fixed and wave frames of reference, respectively.

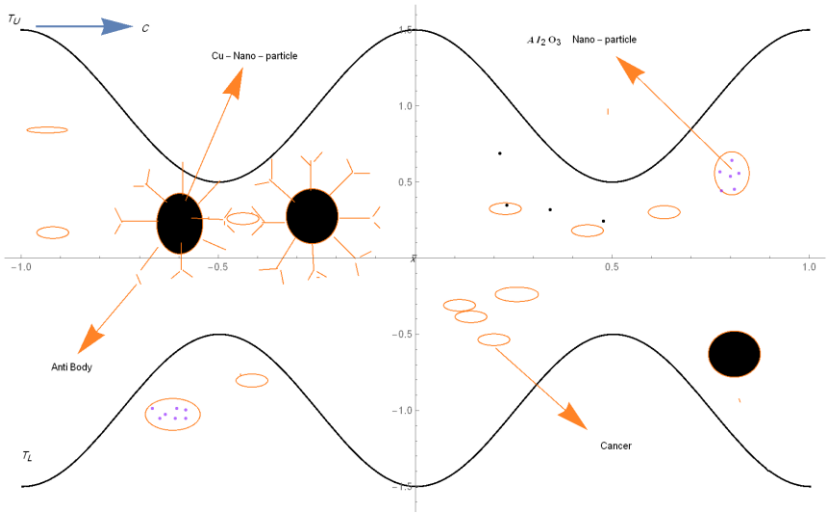

Fig . 1. Hybrid Nano fluid flow due to peristaltic waves with the same amplitude (a) on the walls of a two-dimensional symmetric channel.

The governing equations of the hybrid Nano fluid in a symmetric channel with different shapes of nanoparticles in a moving frame for mass ,momentum and energy are followed by :-

$$\frac{\partial u}{\partial x} + \frac{\partial v}{\partial y} = 0,$$

$$\rho_{hnf}\left[u\frac{\partial u}{\partial x} + v\frac{\partial u}{\partial y}\right] = -\frac{\partial p}{\partial x} + \frac{\mu_f}{(1-\phi_1)^{5/2}(1-\phi_2)^{5/2}}\left[\frac{\partial^2 u}{\partial x^2} + \frac{\partial^2 u}{\partial y^2}\right],$$

$$\rho_{hnf}\left[u\frac{\partial v}{\partial x} + v\frac{\partial v}{\partial y}\right] = -\frac{\partial p}{\partial y} + \frac{\mu_f}{(1-\phi_1)^{5/2}(1-\phi_2)^{5/2}}\left[\frac{\partial^2 v}{\partial x^2} + \frac{\partial^2 v}{\partial y^2}\right], \quad (2.3)$$

$$(\rho C_p)_{hnf}\left[u\frac{\partial T}{\partial x} + v\frac{\partial T}{\partial y}\right] = K_{bf}\frac{K_{s_2} + (m-1)K_{bf} - (m-1)\phi_2(K_{bf} - K_{s_2})}{K_{s_2} + (m-1)K_{bf} + \phi_2(K_{bf} - K_{s_2})}\left[\frac{\partial^2 T}{\partial x^2} + \frac{\partial^2 T}{\partial y^2}\right],$$

Where μ_{hnf}, ρ_{hnf} , C_p and T are the effective dynamic viscosity of the hybrid Nano fluid, effective density of the hybrid Nano fluid, specific heat at constant pressure and temperature. We have in the hybrid Nano fluid:-

$$\mu_{hnf} = \frac{\mu_f}{(1-\phi_1)^{5/2}(1-\phi_2)^{5/2}},$$

$$(\rho C_p)_{hnf} = (1-\phi_2)\left\{(1-\phi_1)(\rho C_p)_f + (\rho C_p)_{s_1}\phi_1\right\} + \phi_2(\rho C_p)_{s_2},$$

$$\rho_{hnf} = (1-\phi_2)\{(1-\phi_1)\rho_f + \rho_{s_1}\phi_1\} + \phi_2\rho_{s_2},$$

$$K_{hnf} = K_{bf}\frac{K_{s_2}+(m-1)K_{bf}-(m-1)\phi_2(K_{bf}-K_{s_2})}{K_{s_2}+(m-1)K_{bf}+\phi_2(K_{bf}-K_{s_2})},$$

$$K_{bf} = K_f\frac{K_{s_1}+(n-1)K_f-(n-1)\phi_1(K_f-K_{s_1})}{K_{s_1}+(n-1)K_f+\phi_1(K_f-K_{s_1})},$$

We have from this relations m, n are the shape factor of Cu and Al_2O_3 nanoparticles respectively .Also $K_f, K_{bf}, K_{s_1}, K_{s_2}$, ϕ_1 , ϕ_2 , μ_f , ρ_f , $(C_p)_f$, ρ_{s_1} , ρ_{s_2} , $(C_p)_{s_1}$ and $(\rho C_p)_{s_2}$ are thermal conductivity of the base fluid (blood) , thermal conductivity of Al_2O_3 -nanofluid , thermal conductivity of Al_2O_3 , thermal conductivity of Cu ,volume fraction of Al_2O_3 nanoparticles , volume fraction of Cu nanoparticles , the base fluid viscosity , the base fluid density , specific heat , the density of Al_2O_3 , the density of Cu , specific heat of Al_2O_3 nanoparticles and specific heat of Cu nanoparticles.

The following table shows the thermo- physical properties of base fluid (blood) and nano particles Cu and Al_2O_3.

Table 1. Thermo-physical properties of base fluid (Blood) & (Water) and nanoparticles Al_2O_3 and Cu

Physical properties	Blood / base fluid	Water/base fluid	$Al_2O_3(\phi_1)$	Cu(ϕ_2)
$\rho\ (kg\ m^{-3})$	1050	997	3970	8933
$C_p(J\ kg^{-1}\ K^{-1})$	3617	4180	765	385
$K(W\ m^{-1}\ K^{-1})$	0.25	0.6071	40	400

3 Dimensionless analysis and wall transformation: -

We define the non-dimensional variables: -

$x = \lambda x^*,\ y = dy^*,\ u = cu^*,\ v = \frac{cd}{\lambda}v^*,\ p = \frac{\mu_f c\,\lambda}{d^2}p^*,\ t = \frac{\lambda}{c}t^*,\ S = \frac{s}{d},$
$\psi = cd\,\psi^*,$

$$T = T_u + \theta(T_l - T_u) \tag{2.4}$$

Where ψ is the stream function { $u = \psi_y$, $v = -\psi_x$ } and λ is the wavelength.

By substitution in (2.3) we get (dropping the stars) :-

$$R_e E_1 E_2 \delta\left(\psi_y\psi_{yx} - \psi_x\psi_{yy}\right) = -E_2 p_x + \psi_{yyy} + \delta^2\psi_{yxx}\,, \tag{2.5}$$

$$R_e E_1 E_2 \delta^3\left(\psi_y\psi_{xx} - \psi_x\psi_{yx}\right) = E_2 p_y + \delta^2(\psi_{xyy} + \delta^2\psi_{xxx}), \tag{2.6}$$

$$\delta\left(\psi_y\theta_x - \psi_x\theta_y\right) = \frac{\alpha_{hnf}}{\alpha_f}\frac{1}{P_r R_e}(\delta^2\theta_{xx} + \theta_{yy})\,, \tag{2.7}$$

Were:

$\delta(\text{wave number}) = \frac{d}{\lambda},\ R_e = \frac{cd}{\nu_f}$ (Reynolds number),

$P_r = \frac{\nu_f}{\alpha_f}$ (Prandtl number)

$\nu_f = \frac{\mu_f}{\rho_f}$ (kinematics viscosity of the base fluid(blood))

$$E_1 = (1-\phi_2)\left\{1-\left(1-\frac{\rho_{s_1}}{\rho_f}\right)\phi_1\right\}+\phi_2\frac{\rho_{s_2}}{\rho_f},$$

$$E_2 = (1-\phi_1)^{5/2}(1-\phi_2)^{5/2}$$

The subscripts x, y refers to the corresponding partial differentiation as long as in what follows. In this paper we study the effects of inertia and curvature at second order with respect to of δ

We can eliminate the pressure from the previous equations (2.5) and (2.6) by cross differentiation so the equations (2.5), (2.6) and (2.7) become: -

$$R_e E_1 E_2 \delta\left(\nabla^2\psi_x - \psi_x\nabla^2\psi_y\right) = \psi_{yyyy} + 2\delta^2\psi_{yyxx} + \delta^4\psi_{xxxx}),$$

$$\delta\left(\psi_y\theta_x - \psi_x\theta_y\right) = \frac{\alpha_{hnf}}{\alpha_f}\frac{1}{P_r R_e}\nabla^2\theta \qquad (2.7)$$

Where $\nabla^2 = \delta^2\frac{\partial^2}{\partial x^2} + \frac{\partial^2}{\partial y^2}$, we introduce the boundary conditions for the flow by

$$\psi = \frac{q}{2} \text{ at } y = \eta = 1 + S(x) \quad , \quad \theta = 0$$

$$\psi = -\frac{q}{2} \text{ at } y = -\eta = -1 - S(x) \quad , \quad \theta = 1 \qquad (2.8)$$

$$\psi_y = -1 \text{ at } y = \eta \text{ and } y = -\eta$$

Where q represents the non-dimensional flow rate in the wave frame at any axial station of the symmetric channel.

Introducing the transformation of the domain of the variable cross section symmetric channel into a channel with straight walls by

$$\zeta = x \qquad \xi = \frac{y}{\eta(x)} \tag{2.9}$$

These relations transform the channel walls $y = \eta(x)$ and $y = -\eta(x)$ into $\xi = \pm 1$ From equation (2.7) we note that $\eta(x)$ and $-\eta(x)$ it must belong to the class of 4th order continuously differentiable functions.

Then from the equations (2.7) and (2.9) we get

$$\frac{R_e E_1 E_2 \delta}{\eta}\left(\psi_\xi \overline{\nabla}^2 \psi_\zeta - \psi_\zeta \overline{\nabla}^2 \psi_\xi\right) = \overline{\nabla}^2 \overline{\nabla}^2 \psi\ , \tag{2.10}$$

$$\frac{\delta}{\eta}\left(\psi_\xi \theta_\zeta - \psi_\zeta \theta_\xi\right) = \frac{\alpha_{hnf}}{\alpha_f}\frac{1}{P_r R_e}\ \overline{\nabla}^2 \theta\ . \tag{2.11}$$

Where:

$$\overline{\nabla}^2 = \left(\frac{1}{\eta^2} + \delta^2 \xi^2 \frac{\eta'^2}{\eta^2}\right)\frac{\partial^2}{\partial \xi^2} + \delta^2 \frac{\partial^2}{\partial \zeta^2} - 2\delta^2 \xi \frac{\eta'}{\eta}\ \frac{\partial^2}{\partial \zeta \partial \xi} + \left(2\delta^2 \xi \frac{\eta'^2}{\eta^2} - \delta^2 \xi \frac{\eta''}{\eta}\right)\frac{\partial}{\partial \xi} \tag{2.12}$$

Where the prime ($'$) refers to the ordinary differentiation with respect to ζ .in this case the corresponding boundary conditions on the walls are

$$\psi = \frac{q}{2} \quad \text{at } \xi = 1 \quad , \quad \theta = 0$$

$$\psi = -\frac{q}{2} \quad \text{at } \xi = -1 \quad , \quad \theta = 1 \tag{2.13}$$

$$\psi_\xi = -\eta \quad \text{at } \xi = \pm 1,$$

Also , the velocity components can be expressed as follow

$$u = \frac{1}{\eta}\,\psi_\xi \quad , \quad v = -\,\psi_\zeta + \xi\,\frac{\eta'}{\eta}\,\psi_\xi$$

Now, we show an asymptotic method of obtaining the solutions (2.10) and (2.11) satisfying the corresponding the previous boundary conditions (2.13)

3 Flow Field: -

In this section we adopt a perturbation method with respect to wave number (δ) as the parameter, is developed.

stream function (ψ) and Heat transfer (θ)

we can write the stream function ψ as follows

$$\psi = \sum_{n=0}^{\infty} \delta^n\,\psi_n, \qquad \theta = \sum_{n=0}^{\infty} \delta^n\,\theta_n \tag{3.1}$$

This expansion takes into account both inertia (R_e) and curvature (δ) effects up to second order so, the method described in this paper is different from what is mentioned in Jaffrin [11] , Manton [13] and Usha and Ramachandra Rao [14]

The equations (2.10) and (2.11) that we obtained through the domain transformation are becoming very complex , but we have the boundary condition $\xi = \pm 1$ on the walls are very much simplified so, we can find the solution these equations in closed form easily .we can substitute from (3.1) in the equations (2.10) ,(2.11) and (2.12) and collecting terms of equal powers with respect to (δ).we get the following sets of equations :-

0th order (δ^0) :-

$$\frac{1}{\eta^4}\,\psi_{0\xi\xi\xi\xi} = 0 \Longrightarrow \psi_{0\xi\xi\xi\xi} = 0\,,\ \frac{\alpha_{hnf}}{\alpha_f}\frac{1}{P_r\,R_e}\frac{1}{\eta^2}\,\theta_{0\xi\xi} = 0 \qquad (3.2)$$

Boundary conditions:-

$$\psi_0(-1) = -\frac{q}{2}, \qquad \theta_0(-1) = 1$$

$$\psi_0(1) = \frac{q}{2}\ , \qquad \theta_0(1) = 0\ ,$$

$$\psi_{0\xi} = -\eta \quad \text{at} \quad \xi = -1 \qquad (3.3)$$

$$\psi_{0\xi} = -\eta \quad \text{at} \quad \xi = 1$$

1st order (δ^1) :-

$$\psi_{1\xi\xi\xi\xi} = R_e E_1 E_2 \eta\left[\ \psi_{0\xi}\psi_{0\zeta\xi\xi} - \psi_{0\zeta}\psi_{0\xi\xi\xi}\right] - 2R_e E_1 E_2 \eta'[\psi_{0\xi}\psi_{0\xi\xi}]\,,$$

$$\frac{\alpha_{hnf}}{\alpha_f}\frac{1}{P_r\,R_e}\frac{1}{\eta^2}\,\theta_{1\xi\xi} = \frac{1}{\eta}(\psi_{0\xi}\theta_{0\zeta} - \psi_{0\zeta}\theta_{0\xi}) \qquad (3.4)$$

Boundary conditions :-

$$\psi_1(-1) = 0,\ \theta_1(-1) = 0$$

$$\psi_1(1) = 0,\ \theta_1(1) = 0$$

$$\psi_{1\xi} = 0 \quad \text{at} \quad \xi = -1 \qquad (3.5)$$

$$\psi_{1\xi} = 0 \quad \text{at} \quad \xi = 1$$

2nd order (δ^2) :-

$$\psi_{2\xi\xi\xi\xi} = R_e E_1 E_2 \eta\{\psi_{0\xi}\psi_{1\zeta\xi\xi} - \psi_{0\zeta}\psi_{1\xi\xi\xi} + \psi_{1\xi}\psi_{0\zeta\xi\xi} - \psi_{1\zeta}\psi_{0\xi\xi\xi}\} - 2R_e E_1 E_2 \eta'\{\psi_{0\xi}\psi_{1\xi\xi} + \psi_{1\xi}\psi_{0\xi\xi}\} - 2\eta^2\psi_{0\zeta\zeta\xi\xi} + 8\eta\eta'\psi_{0\zeta\xi\xi} - \{12\eta'^2 - 4\eta\eta''\}\psi_{0\xi\xi} + 4\xi\eta\eta'\psi_{0\zeta\xi\xi\xi}$$

$$-2\{6\xi\eta'^2 - \xi\eta\eta''\}\psi_{0\xi\xi\xi}$$

$$\theta_{2\xi\xi} = \frac{1}{4}\frac{(\eta\eta'^2+\eta^2\eta'')}{(\frac{\alpha_{hnf}}{\alpha_f}\frac{1}{Pr\,Re})^2}\left[\frac{\xi^3}{6}-\frac{\xi^5}{20}-7\frac{\xi}{6}\right]\left[\left(\frac{\eta}{2}+\frac{3q}{4}\right)-\xi^2\left(\frac{3\eta}{2}+\frac{3q}{4}\right)\right]+$$

$$\frac{\eta^2\eta'^2}{8(\frac{\alpha_{hnf}}{\alpha_f}\frac{1}{Pr\,Re})^2}(\xi^3-\xi)\left[\frac{\xi^2}{2}-\frac{\xi^4}{4}-\frac{7}{6}\right]+\frac{\eta\,R_eE_1E_2}{2(\frac{\alpha_{hnf}}{\alpha_f}\frac{1}{Pr\,Re})}\xi\left[\frac{3}{280}\left(2\eta\eta'^2+\eta^2\eta''\right)+\right.$$

$$\left.\frac{11}{560}q\left(\eta'^2+\eta\eta''\right)+\frac{3}{224}q^2\eta''\right]-\frac{\eta\,R_eE_1E_2}{2(\frac{\alpha_{hnf}}{\alpha_f}\frac{1}{Pr\,Re})}\xi^3\left[\frac{1}{35}\left(2\eta\eta'^2+\eta^2\eta''\right)+\right.$$

$$\left.\frac{27}{560}q\left(\eta'^2+\eta\eta''\right)+\frac{33}{1120}q^2\eta''\right]+\frac{\eta\,R_eE_1E_2}{2(\frac{\alpha_{hnf}}{\alpha_f}\frac{1}{Pr\,Re})}\xi^5\left[\frac{1}{40}\left(2\eta\eta'^2+\eta^2\eta''\right)+\right.$$

$$\left.\frac{3}{80}q\left(\eta'^2+\eta\eta''\right)+\frac{3}{160}q^2\eta''\right]-\frac{\eta\,R_eE_1E_2}{2(\frac{\alpha_{hnf}}{\alpha_f}\frac{1}{Pr\,Re})}\xi^7\left[\frac{1}{140}\left(2\eta\eta'^2+\eta^2\eta''\right)+\right.$$

$$\left.\frac{1}{112}q\left(\eta'^2+\eta\eta''\right)+\frac{3}{1120}q^2\eta''\right]-\frac{\xi\eta\eta''}{2}+\xi\eta'^2 \qquad (3.6)$$

Boundary conditions:-

$$\psi_2(-1)=0\,,\theta_2(-1)=0$$

$$\psi_2(1)=0$$

$$\theta_2(1)=0$$

$$\psi_{2\xi}=0 \quad \text{at} \quad \xi=-1 \qquad (3.7)$$

$$\psi_{2\xi}=0 \quad \text{at} \quad \xi=1$$

Then the solutions of 0th order (δ^0) , 1st order (δ^1) and 2nd order (δ^2) satisfying the corresponding boundary conditions are :-

$$\psi_0=\frac{\xi}{2}\left(\eta+\frac{3q}{2}\right)-\frac{\xi^3}{2}\left(\eta+\frac{q}{2}\right),\ \theta_0=\frac{1}{2}(1-\xi)$$

$$\psi_1 = R_e E_1 E_2 \left(\frac{3\eta^2\eta'}{280} + \frac{11q\eta\eta'}{560} + \frac{3q^2\eta'}{224}\right)\xi - R_e E_1 E_2 * \left(\frac{\eta^2\eta'}{35} + \frac{27q\eta\eta'}{560} + \frac{33\,q^2\eta'}{1120}\right)\xi^3 + R_e E_1 E_2 (\frac{\eta^2\eta'}{40} + \frac{3q\eta\eta'}{80} + \frac{3q^2\eta'}{160})\xi^5 - R_e E_1 E_2 (\frac{\eta^2\eta'}{140} + \frac{q\eta\eta'}{112} + \frac{3q^2\eta'}{1120})\xi^7),$$

$$\theta_1 = \frac{\eta\eta'}{4(\frac{\alpha_{hnf}}{\alpha_f}\frac{1}{Pr\,Re})}\left[\frac{\xi^3}{6} - \frac{\xi^5}{20} - 7\frac{\xi}{6}\right]$$

$$\psi_2 = (\frac{f_2}{120} + (R_e E_1 E_2)^2 * (\frac{f_3}{120} + \frac{f_4}{420} + \frac{f_5}{1008} + \frac{f_6}{1980}))\xi - (\frac{f_2}{60} + (R_e E_1 E_2)^2 * (\frac{f_3}{60} + \frac{f_4}{280} + \frac{f_5}{756} + \frac{f_6}{1584}))\xi^3 + (\frac{f_2 + (R_e E_1 E_2)^2 * f_3}{120})\xi^5 + \frac{(R_e E_1 E_2)^2 * f_4}{840}\xi^7 + \frac{(R_e E_1 E_2)^2 * f_5}{3024}\xi^9 + \frac{(R_e E_1 E_2)^2 * f_6}{7920}\xi^{11}),$$

$$\theta_2 = \frac{1}{4}\frac{\left(\eta\eta'^2 + \eta^2\eta''\right)}{\left(\frac{\alpha_{hnf}}{\alpha_f}\frac{1}{Pr\,Re}\right)^2}\left(\frac{\eta}{2} + \frac{3q}{4}\right)\left[\frac{\xi^5}{120} - \frac{\xi^7}{840} - 7\frac{\xi^3}{36} + \frac{59\xi}{315}\right] - \frac{1}{4}\frac{\left(\eta\eta'^2 + \eta^2\eta''\right)}{\left(\frac{\alpha_{hnf}}{\alpha_f}\frac{1}{Pr\,Re}\right)^2}\left(3\frac{\eta}{2} + \frac{3q}{4}\right)\left[\frac{\xi^7}{252} - \frac{\xi^9}{1440} - 7\frac{\xi^5}{120} + \frac{37\,\xi}{672}\right] + \frac{\eta^2\eta'^2}{8\left(\frac{\alpha_{hnf}}{\alpha_f}\frac{1}{Pr\,Re}\right)^2}\left[\frac{\xi^7}{56} - \frac{\xi^9}{288} - \frac{\xi^5}{12} - 7\frac{\xi^3}{36} + \frac{59\,\xi}{224}\right] + \frac{\eta\,R_e E_1 E_2}{12\left(\frac{\alpha_{hnf}}{\alpha_f}\frac{1}{Pr\,Re}\right)}(\xi^3 - \xi)\left[\frac{3}{280}\left(2\eta\eta'^2 + \eta^2\eta''\right) + \frac{11}{560}q\left(\eta'^2 + \eta\eta''\right) + \frac{3}{224}q^2\eta''\right] - \frac{\eta\,R_e E_1 E_2}{40\left(\frac{\alpha_{hnf}}{\alpha_f}\frac{1}{Pr\,Re}\right)}(\xi^5 - \xi)\left[\frac{1}{35}\left(2\eta\eta'^2 + \eta^2\eta''\right) + \frac{27}{560}q\left(\eta'^2 + \eta\eta''\right) + \frac{33}{1120}q^2\eta''\right] + \frac{\eta\,R_e E_1 E_2}{84\left(\frac{\alpha_{hnf}}{\alpha_f}\frac{1}{Pr\,Re}\right)}(\xi^7 - \xi)\left[\frac{1}{40}\left(2\eta\eta'^2 + \eta^2\eta''\right) + \frac{3}{80}q\left(\eta'^2 + \eta\eta''\right) + \frac{3}{160}q^2\eta''\right] - \frac{\eta\,R_e E_1 E_2}{144\left(\frac{\alpha_{hnf}}{\alpha_f}\frac{1}{Pr\,Re}\right)}(\xi^9 - \xi)\left[\frac{1}{140}\left(2\eta\eta'^2 + \eta^2\eta''\right) + \frac{1}{112}q\left(\eta'^2 + \eta\eta''\right) + \frac{3}{1120}q^2\eta''\right] - \frac{\eta\eta''}{12}(\xi^3 - \xi) + \frac{\eta'^2}{6}(\xi^3 - \xi)$$

The expressions for f_1 , f_2 , f_3 , f_4 , f_5 are given in Appendix (1) . solutions of 0^{th} order (δ^0) , 1^{st} order (δ^1) and 2^{nd} order (δ^2).....

The flux at any axial station in the fixed frame $(\bar{x}, \bar{y})$ is

$$Q = \int_{-\eta}^{\eta}(u+1)\,dy = \int_{-\eta}^{\eta}(u)\,dy + \int_{-\eta}^{\eta} dy = q + 2\eta .$$

Also, the time mean flow rate (the quantity of practical interest)

$$\bar{Q} = \frac{1}{T}\int_0^T Q\,dt = \frac{1}{T}\int_0^T (q+2\eta)\,dt = q + 2 ,$$

As η is periodic function with period $T\left(=\frac{\lambda}{c}\right)$.

4 Pumping Characteristics:-

In peristaltic motion the pumping is always characterized by the relation between the time mean flow rate $\bar{Q}$ to the pressure difference Δp at the ends of the channel. With respect to the pressure

$$p = \sum_{n=0}^{\infty} \delta^n\, p_n \qquad (4.1)$$

From equations (2.5) & (2.6), we get p_0 , p_1 and p_2 with the same the previous technique in stream function and heat transfer

0^{th} order (δ^0) :-

$$p_{0x} = \frac{1}{E_2}\psi_{0yyy} \qquad (4.2)$$

$$p_{0y} = 0 .$$

1^{th} order (δ^1) :-

$$p_{1x} = \frac{1}{E_2}\{\psi_{1yyy} - R_e E_1 E_2(\psi_{0y}\psi_{0yx} - \psi_{0x}\psi_{0yy})\} \quad (4.3)$$

$$p_{1y} = 0 .$$

2nd order (δ^2) :-

$$p_{2x} = \frac{1}{E_2}\{\psi_{2yyy} + \psi_{0yxx}\} - R_e E_1(\psi_{0y}\psi_{1yx} + \psi_{1y}\psi_{0yx} - \psi_{0x}\psi_{1yy} - \psi_{1x}\psi_{0yy}), \quad (4.4)$$

$$p_{2y} = -\frac{1}{E_2}\psi_{0xyy}$$

We can calculate p_0 , p_1 and p_2 from expressions ψ_0 , ψ_1 and ψ_2 in the (x, y) coordinate by using the transformation which transform the domain of variable cross section a symmetric channel into a channel with straight walls

$$p_{0x} = -\frac{3q}{2E_2\eta^3} - \frac{3}{E_2\eta^{2'}}, \quad p_{0y} = 0 \quad (4.5)$$

$$p_{1x} = E_1 R_e\{\frac{27q^2\eta'}{70\ \eta^3} + \frac{3q\eta'}{35\eta^2} - \frac{6\eta'}{35\ \eta}\} \quad p_{1y} = 0 \quad (4.6)$$

$$p_{2y} = -\frac{9qy\eta'}{2E_2\eta^4} - \frac{6y\eta'}{E_2\eta^3},$$

$$p_{2x} = -\frac{11\ {E_1}^2E_2{R_e}^2\ \eta'^2}{1225} + \frac{9qy^2\eta'^2}{E_2\eta^5} + \frac{9y^2\eta'^2}{E_2\eta^4} - \frac{21q\eta'^2}{10E_2\eta^3} + \frac{78\ {E_1}^2E_2{R_e}^2q^3\eta'^2}{13475\eta^3} - \frac{18\eta'^2}{5E_2\eta^2} + \frac{13\ {E_1}^2E_2{R_e}^2q^2\eta'^2}{13475\eta^2} - \frac{2\ {E_1}^2E_2{R_e}^2q\eta'^2}{175\eta} - \frac{127\ {E_1}^2E_2{R_e}^2q\eta''}{11550} - \frac{9qy^2\eta''}{4E_2\eta^4} - \frac{3y^2\eta''}{E_2\eta^3} + \frac{3q\eta''}{20E_2\eta^2} - \frac{117\ {E_1}^2E_2{R_e}^2q^3\eta''}{26950\eta^2} + \frac{6\eta''}{5E_2\eta} - \frac{158\ {E_1}^2E_2{R_e}^2q^2\eta''}{13475\eta} - \frac{166\ {E_1}^2E_2{R_e}^2\eta\ \eta''}{40425} . \quad (4.7)$$

Where the prime ($'$) refers to the ordinary differentiation with respect to x. From these relations we have the pressure in x and y direction is a function of x, y up to second order (δ^2), also we note that both p_{0y} and p_{1y} equal zero but p_{2y} not equal zero.

We define the difference of the pressures averaged over the cross section at axial stations $x = 0$ & $x = L$ (length of the channel) the mean pressure difference (Δp_L),

$$\Delta p_L = \frac{1}{2\eta_{x=0}} \int_{-\eta_{x=0}}^{\eta_{x=0}} p(0)dy - \frac{1}{2\eta_{x=L}} \int_{-\eta_{x=L}}^{\eta_{x=L}} p(L)dy . \quad (4.8)$$

We assume that L is an integral multiple of λ, so the pressure difference(Δp) over $\lambda = 1$ is

$$\Delta p = \frac{1}{\eta_{x=0}} \int_{-\eta_{x=0}}^{\eta_{x=0}} (\int_0^{\lambda} \frac{\partial p}{\partial x} dx)dy. \quad (4.9)$$

Where η is periodic with period λ . from equations (4.2), (4.3),(4.4),(4.5),(4.6),(4.7) and (4.9)

$$\Delta p = (\Delta p)_0 + \delta\,(\Delta p)_1 + \delta^2(\Delta p)_2 + O(\delta^3).$$

Where :-

$$(\Delta p)_0 = \frac{1}{\eta_{x=0}} \int_{-\eta_{x=0}}^{\eta_{x=0}} (\int_0^{\lambda} p_{0x}\, dx)dy,$$

$$(\Delta p)_1 = \frac{1}{\eta_{x=0}} \int_{-\eta_{x=0}}^{\eta_{x=0}} (\int_0^{\lambda} p_{1x}\, dx)dy, \quad (4.10)$$

$$(\Delta p)_2 = \frac{1}{\eta_{x=0}} \int_{-\eta_{x=0}}^{\eta_{x=0}} (\int_0^{\lambda} p_{2x}\, dx)dy.$$

The different integrals appearing in (4.10) are given in appendix (2) which evaluated using the software package Mathematica 4.1and are presented in appendix (3) .in this paper we prescribe the peristaltic waves on the wall by

$$\eta = 1 + a\ \cos 2\pi x, \quad \text{Upper wall} \quad (4.11)$$

$-\eta = -1 - a\ \cos 2\pi x$ Lower wall

Where a is dimensionless amplitude of the wave .after calculating all the integrals we get the pressure rise over $\lambda = 1$ which is independent of y.

$$(\Delta p)_0 = \frac{-6}{E_2}\{\frac{1}{(1-a^2)^{\left(\frac{3}{2}\right)}} + \frac{(2+a^2)q}{4(1-a^2)^{\left(\frac{5}{2}\right)}}\},$$

$$(\Delta p)_1 = 0,$$

(4.12)

$$(\Delta p)_2 = \frac{-788}{40425}\pi^2 a^2\ E_2\ (R_e E_1)^2 - \frac{16}{175}\pi^2\ q\ E_2\ (R_e E_1)^2\left(1-\sqrt{1-a^2}\right) - \frac{232}{2695}\pi^2 E_2\ q^2 (R_e E_1)^2\left(-1+\frac{1}{\sqrt{1-a^2}}\right)$$
$$-\frac{156}{13475}\ \pi^2 a^2 q^3 E_2 (R_e E_1)^2 \frac{1}{(1-a^2)^{\left(\frac{3}{2}\right)}} - \frac{96}{5E_2}\pi^2\ \left(-1+\frac{1}{\sqrt{1-a^2}}\right)$$
$$-\frac{36}{5E_2}\ \pi^2 a^2 q \frac{1}{(1-a^2)^{\left(\frac{3}{2}\right)}}\ .$$

We can write the pressure difference (Δp) as follow

$$\Delta p = \varphi_0 + \varphi_1 q + \varphi_2 q^2 + \varphi_3 q^3 + O(\delta^3).$$

Where

$$\varphi_0 = 2\{\frac{-3}{E_2(1-a^2)^{\left(\frac{3}{2}\right)}} - 0.009744\ \pi^2 a^2 \delta^2 E_2 (R_e E_1)^2 - \frac{48}{5E_2}\pi^2\delta^2\left(-1+\frac{1}{\sqrt{1-a^2}}\right)\},$$

$$\varphi_1 = 2\{\frac{-3(2+a^2)}{4E_2(1-a^2)^{\left(\frac{5}{2}\right)}} - \frac{18}{5E_2}\ \frac{\pi^2 a^2 \delta^2}{(1-a^2)^{\left(\frac{3}{2}\right)}} - 0.045708\ \pi^2 E_2 (R_e E_1)^2 \delta^2\left(1-\sqrt{1-a^2}\right)\},$$

$$\varphi_2 = 2\{-0.043044\ \pi^2 E_2\ \delta^2 (R_e E_1)^2 \left(-1 + \frac{1}{\sqrt{1-a^2}}\right)\},$$

$$\varphi_3 = 2\{-0.005792\ \pi^2 a^2 \delta^2 E_2 (R_e E_1)^2 \frac{1}{(1-a^2)^{\left(\frac{3}{2}\right)}}\}.$$

We want to express the pressure difference in terms the mean flow rate $\bar{Q} = (q + 2)$ up to the 2nd order of δ.we can write the pressure difference

$$\Delta p = \mathcal{E}_0 + \mathcal{E}_1 \bar{Q} + \mathcal{E}_2 \bar{Q}^2 + \mathcal{E}_3 \bar{Q}^3, \qquad (3.21)$$

Where

$$\boldsymbol{\mathcal{E}_0 = \varphi_0 - 2\varphi_1 + 4\varphi_2 - 8\varphi_3,}$$
$$\boldsymbol{\mathcal{E}_1 = \varphi_1 - 4\varphi_2 + 12\varphi_3,}$$
$$\boldsymbol{\mathcal{E}_2 = \varphi_2 - 6\varphi_3,}$$
$$\boldsymbol{\mathcal{E}_3 = \varphi_3.}$$

We note that the coefficients $\boldsymbol{\varphi_0, \varphi_1, \varphi_2}$ and $\boldsymbol{\varphi_3}$ are functions of the non-dimensional parameters $\boldsymbol{\delta}$, $\boldsymbol{a}$ and $\boldsymbol{R_e}$. From the relations (4.12) we note that $\boldsymbol{(\Delta p)_1 = 0}$, then we find no term proportional with $\boldsymbol{R_e}$ .if we put $\boldsymbol{R_e = 0}$, $\boldsymbol{\delta \neq 0}$ we get streamline curvature effects. But if we put $\boldsymbol{\delta = 0}$, $\boldsymbol{R_e \neq 0}$ this case isn't possible .

5 Shear stress at the walls of the channel :-

in this section we describe the shear stress distribution on the upper and lower walls of the channel which is a physical quantity of interest in the flows of uniform cross section

With respect to upper wall at $y = \eta(x)$, the tangential stress of the symmetric channel is given by

$$T = (\sigma_{xy}\left\{1 - \left\{\frac{d\eta}{dx}\right\}^2\right\} + \{\sigma_{yy} - \sigma_{xx}\} * \frac{d\eta}{dx} \quad) \quad / \quad (1 + \left\{\frac{d\eta}{dx}\right\}^2)$$

(5.1)

Where $\boldsymbol{\sigma_{xx}}$, $\boldsymbol{\sigma_{xy}}$ and $\boldsymbol{\sigma_{yy}}$ are stress tensor's components and the shear stress tensor for the motion is

$$\boldsymbol{\sigma_{ij}} = -\boldsymbol{p\delta_{ij}} + \boldsymbol{2\mu e_{ij}},$$

Then

$$\boldsymbol{\sigma_{xx}} = -\boldsymbol{p} + \boldsymbol{2\mu e_{xx}} = -\boldsymbol{p} + \boldsymbol{2\,\mu}\frac{\boldsymbol{\partial u}}{\boldsymbol{\partial x}} == -\boldsymbol{p} + \boldsymbol{2\,\mu\psi_{yx}},$$

$$\sigma_{yy} = -p + 2\mu e_{yy} = -p + 2\,\mu\frac{\partial v}{\partial y} = -p - 2\,\mu\psi_{xy}, \qquad (5.2)$$

$$\sigma_{xy} = 2\mu e_{xy} = \mu\left(\frac{\partial u}{\partial y} + \frac{\partial v}{\partial x}\right) = \mu(\psi_{yy} - \psi_{xx}).$$

We introduce the non-dimensional for shear stress distribution

$$T = \frac{\mu c}{d}\tau,$$

$$\tau(x,y) = \tau_0(x,y) + \boldsymbol{\delta}\tau_1(x,y) + \boldsymbol{\delta^2}\tau_2(x,y) + o(\boldsymbol{\delta^3}), \qquad (5.3)$$

Where $\tau_0 = \psi_{0yy}$, $\tau_1 = \psi_{1yy}$, $\tau_2 = \psi_{2yy} - \psi_{0xx} - 2\psi_{0yy}\left(\frac{d\eta}{dx}\right)^2 - 4\psi_{0xy}\left(\frac{d\eta}{dx}\right)$.

In order to transform (x,y) system to (ζ, ξ), we using the transformation (2.9)

So the shear stress is

$$\tau(\zeta,\xi) = \tau_0(\zeta,\xi) + \boldsymbol{\delta}\tau_1(\zeta,\xi) + \boldsymbol{\delta^2}\tau_2(\zeta,\xi) + o(\boldsymbol{\delta^3}). \qquad (5.4)$$

By substituting for ψ_0, ψ_1, ψ_2 into (5.4), and evaluate at the wall $\xi = 1$, we get

$$\tau(\zeta,\xi) = -\frac{6\xi\left(\frac{q}{4}+\frac{\eta}{2}\right)}{\eta^2} + \delta * \frac{1}{\eta^2}\left(-42R_e\xi^5 e_1e_2\left(\frac{3q^2\eta'}{1120} + \frac{1}{112}q\eta\eta' + \frac{1}{140}\eta^2\eta'\right) + 20R_e\xi^3 e_1e_2\left(\frac{3}{160}q^2\eta' + \frac{3}{80}q\eta\eta' + \frac{1}{40}\eta^2\eta'\right) - 6R_e\xi e_1e_2\left(\frac{33q^2\eta'}{1120} + \frac{27}{560}q\eta\eta' + \frac{1}{35}\eta^2\eta'\right)\right) + \delta^2 *$$

$$\left(\frac{1}{5174400\eta^2}\left(-2\left(-776160q\left(10+\xi(-7+30(-1+\xi)\xi)\right)+3{R_e}^2q^3\xi\left(12333+77\xi^2(-570+612\xi^2-270\xi^4+35\xi^6)\right)e_1^2e_2^2+4\xi\eta\left(-388080\left(4+5\xi(-4+3\xi)\right)+3{R_e}^2q^2\left(4412+1155\xi^2(-19+29\xi^2-17\xi^4+3\xi^6)\right)e_1^2e_2^2+11{R_e}^2e_1^2e_2^2\eta\left(28q\left(24+5\xi^2(-33+63\xi^2-45\xi^4+11\xi^6)\right)+\left(213+7\xi^2(-255+531\xi^2-405\xi^4+110\xi^6)\right)\eta\right)\right)\right){\eta'}^2+\xi\eta\left(-776160q(-11+15\xi^2)+3{R_e}^2q^3\left(9837+77\xi^2(-420+414\xi^2-180\xi^4+25\xi^6)\right)e_1^2e_2^2+4\eta\left(-776160(-2+5\xi^2)+4{R_e}^2q^2\left(3138+385\xi^2(-33+45\xi^2-27\xi^4+5\xi^6)\right)e_1^2e_2^2+{R_e}^2e_1^2e_2^2\eta\left(7q\left(1268+55\xi^2(-111+189\xi^2-141\xi^4+35\xi^6)\right)+2\left(809+77\xi^2(-75+177\xi^2-165\xi^4+50\xi^6)\right)\eta\right)\right)\eta''\right)\right)+o(\boldsymbol{\delta^3}).$$

Similarly we can compute the shear stress at the lower wall at $\xi=-1$.

6 Rate of working of wall of channel :-

We can calculate the energy which pumps fluid through the channel by peristalsis comes from the working of the channel wall against the radial force($\boldsymbol{F}$) exerted by the fluid on the wall of the channel. But the axial force exerted by the fluid it has no effect on the wall due to no axial velocity on the wall of the channel. we consider the motion in the wave frame (x, y)

the radial force($\boldsymbol{F}$) exerted by the fluid on the wall of the channel per unit area acting on the fluid at upper wall at $y = \eta(x)$,

$$\boldsymbol{F}=\{\sigma_{yy}-\sigma_{xy}\delta\frac{d\eta}{dx}\}\quad/\quad\{1+\delta^2\left\{\frac{d\eta}{dx}\right\}^2\}^{1/2}$$

Where the stress tensor **is given by** $\boldsymbol{\sigma_{ij}=-p\delta_{ij}+2\mu e_{ij}}$,

Where σ_{xy} and σ_{yy} are stress tensor's components Then

$$\sigma_{yy} = -p + 2\mu e_{yy} = -p + 2\,\mu\frac{\partial v}{\partial y} = -p - 2\,\mu\psi_{xy},$$

$$\sigma_{xy} = 2\mu e_{xy} = \mu\left(\frac{\partial u}{\partial y} + \frac{\partial v}{\partial x}\right) = \mu(\psi_{yy} - \psi_{xx}).$$

The net rate of working of the wall over a wavelength λ is

$$W = \int_0^{\lambda}\left(\frac{2\pi\eta\mu_f}{\rho_f}\right)F\,dx\ .$$

7. Discussion of the results

7.1. Trapping phenomenon

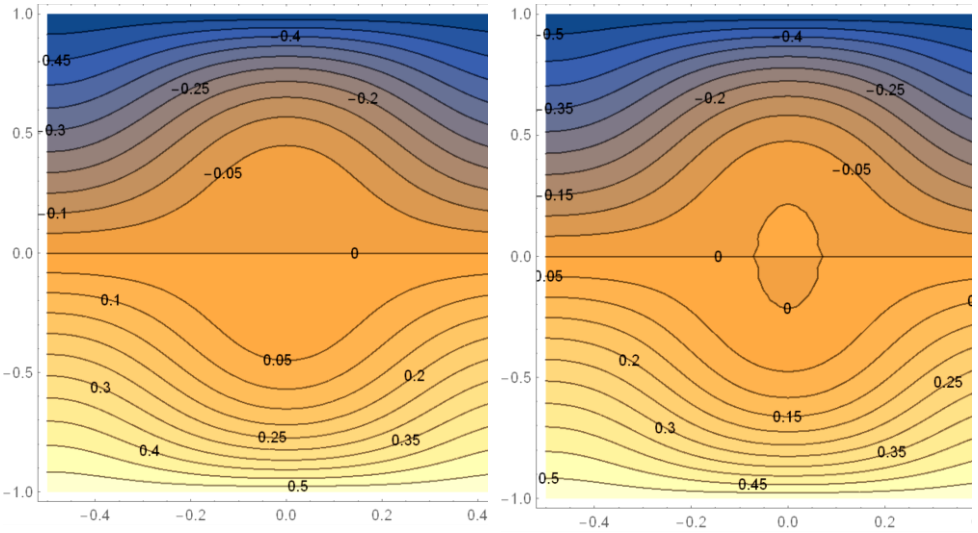

(a) (b)

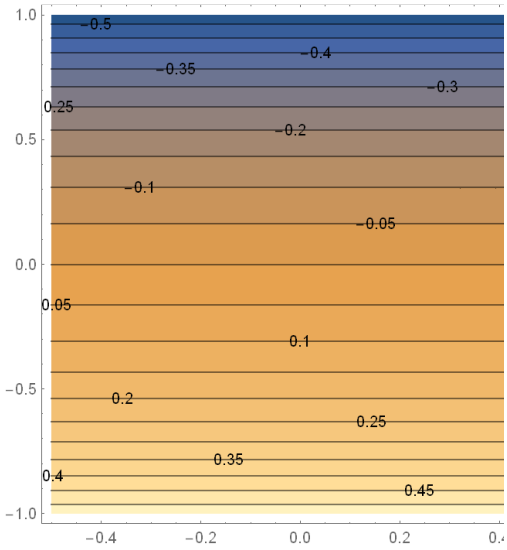

(c)

Fig(1).curvature effects on streamlines for $a = 0.6$, $a = 0$, $q = -1.07$, $R_e = 0$, $\delta = 0$, $\delta = 0.1$, $\phi_1 = 0.1$, $\phi_2 = 0.03$ with (a) $\delta = 0$, $a = 0.6$ - (b) $\delta = 0.1$, $a = 0.6$ - (c) $\delta = 0$, $a = 0$

Trapping is an important phenomenon in peristaltic motion; in a reference frame (moving frame) moving with the wave speed c we observed that the streamlines split to trap a bolus of fluid under certain conditions. We note that the streamline pattern for hybrid nano-fluid With $a = 0.6, q = -1.07, R_e = 0, \delta = 0,$ $\delta = 0.1$, $\phi_1 = 0.1$, $\phi_2 = 0.03$ as shown in Fig (1). The centre streamline $\psi = 0$ split to trap a bolus of hybrid nano-fluid as shown in Fig (1b) for $\delta = 0.1$, but there is no trapped bolus in Fig (1a) at $\delta = 0$, since δ give us the curvature effects .so we deduce the limits of trapping with $\delta = 0$ the details in [23], since $\delta(\text{wave number}) = \frac{d}{\lambda}$ i.e., $\lambda \to \infty$ this mean that there is no wave so we get the behaviour of hybrid nano-

fluid in Poiseuille flow as shown in Fig (1c).so we get the curvature effects is decreasing the minimize limit on $\bar{Q}$ ($\bar{Q} = q + 2$) with respect to the center streamline trapping and this result is compatible with[11] .

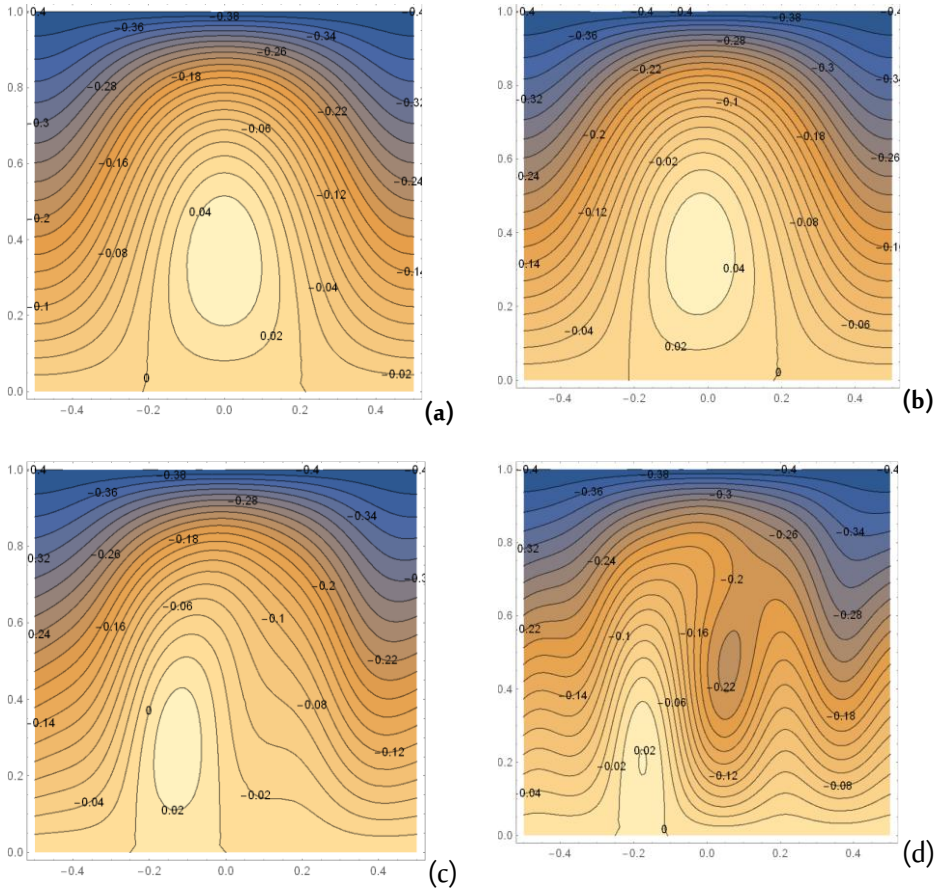

Fig.(2).Inertia & viscous effects on streamlines for $a = 0.7$, $q = -0.8$, $\delta = 0.01$, $\phi_1 = 0.1$, $\phi_2 = 0.03$ with (a) $R_e = 0$, (b) $R_e = 110$, (c) $R_e = 550$, (d) $R_e = 1000$

Fig.(2) shows the effects of inertia force that represented by Reynolds number (R_e) on trapping for $a = 0.7$, $q = -0.8$, $\delta = 0.01$, $\phi_1 = 0.1$, $\phi_2 = 0.03$ .we

find in this figure when inertia forces are non-existent i.e., $R_e = 0$, the streamlines show converting trapping case from symmetric trapped into asymmetric trapped which moving towards the direction of upstream then reduce gradually as shown in Fig .2b, c and d and this result also is compatible with[16] .in this paper we take Reynolds number (R_e) arbitrary so we can choose it very large as in case (d) $R_e = 1000$ we note that there is another eddy on the side of downstream for a channel although the some expect another eddy on the side of downstream for a tube from an engineering perspective only .

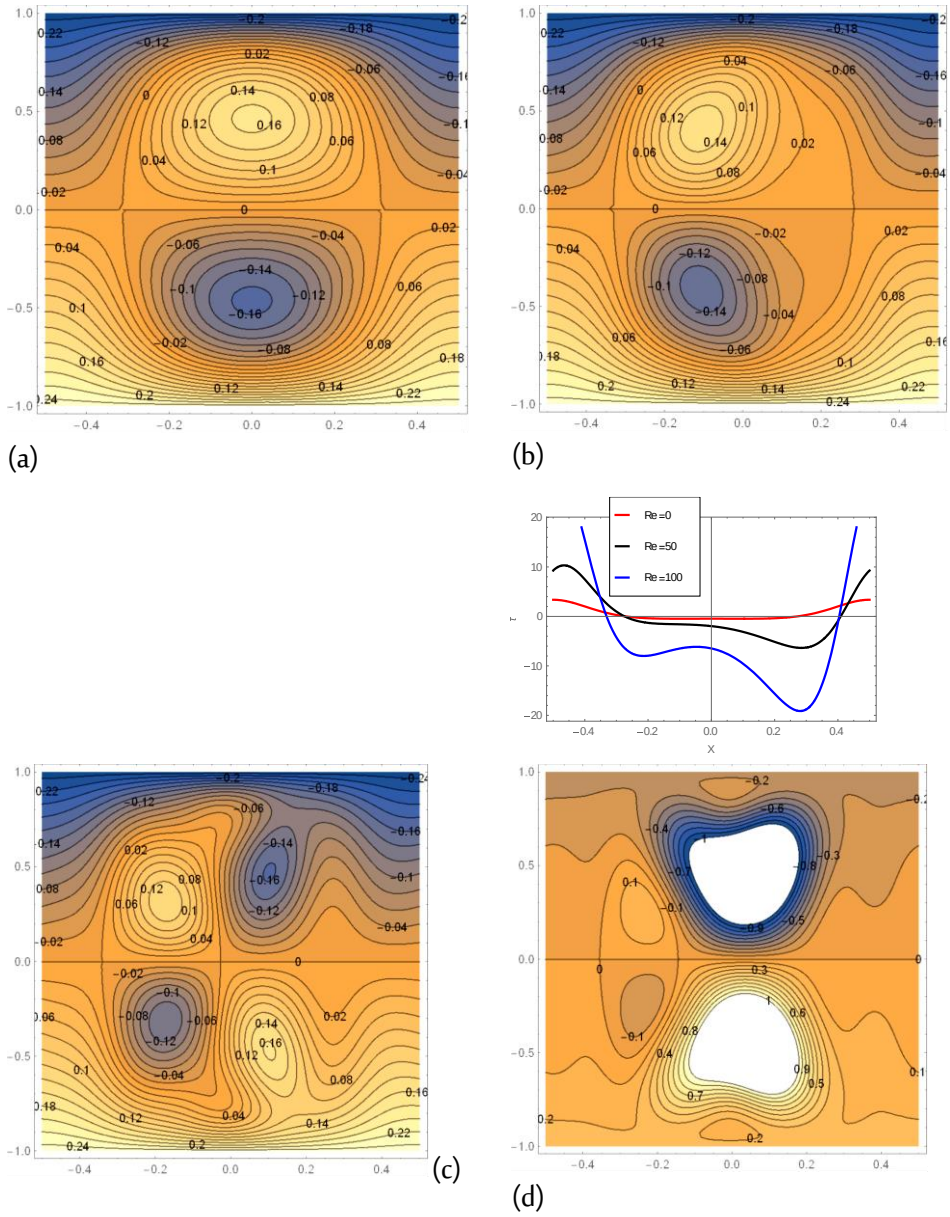

Fig. (3).Inertia & curvature effects on streamlines for $a = 0.7$, $q = -0.5$, $\delta = 0.1$, $\phi_1 = 0.1$, $\phi_2 = 0.03$ with (a) $R_e = 0$, (b) $R_e = 110$, (c) $R_e = 550$, (d) $R_e = 1000$

Fig. (3) Shows inertia force and curvature on the stream lines we must plotted the streamlines for $= 0.7$, $q = -0.5$ with different Reynolds numbers for $\delta = 0.1$ (> 0.01 *as seen in figur* 9) we find in Fig. (3a) variation(asymmetry) in stream lines is caused by the forces of inertia (R_e) and Fig. (3b) we observed that The centre streamline $\psi = 0$ split additionally four stagnation points *as seen in* Fig. (3c) but Fig. (3d) the 2nd eddy growths on the under stream side of the channel whereas Ramachandra Rao and Usha [14] there is The centre streamline $\psi = 0$ spliting in addition to more than two stagnation points.

Shear stress distributions: -

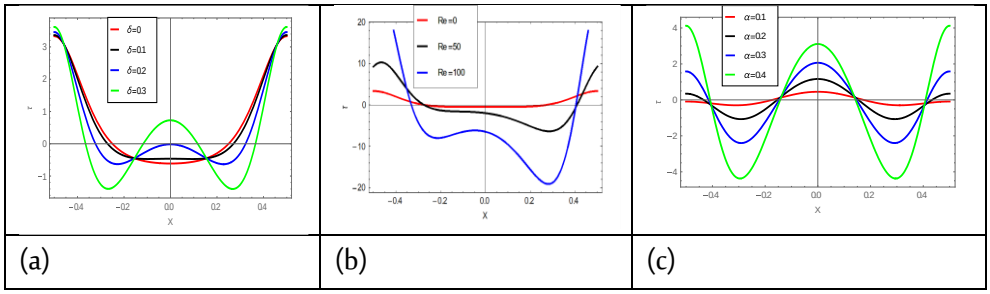

(a) (b) (c)

Fig. (4).Shear stress on the upper wall with $q = -2$, $\phi_1 = 0.1$, $\phi_2 = 0.03$

(a) For various δ (b) For various R_e (c) $R_e =$ For various α

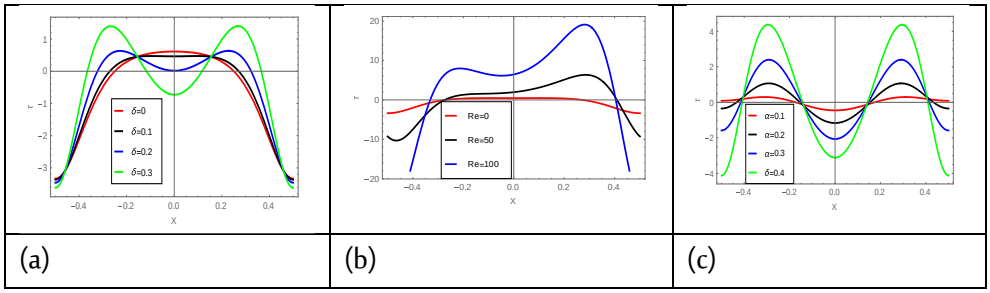

(a) (b) (c)

Fig. (5).Shear stress on the lower wall with $q = -2$, $\phi_1 = 0.1$, $\phi_2 = 0.03$

(a) For various δ (b) For various R_e (c) $R_e =$ For various α

Both Fig. (4) and Fig. (5) show the shear stress distribution at the lower and upper walls of the channel which play an important role in the medical applications .we note that in Fig. (4) shear stress distributions on the upper wall For various curvature effects, inertia forces and the amplitude of the channel . in Fig. (4a) shear stress distributions increases with an increases curvature effects at $X = 0$ in addition to symmetry the shear stress about line $X = 0$ which does not happen in Fig. (4b) at increasing of Reynold's number .Also in Fig. (4c) shear stress distributions increases with an increases values of amplitude of the channel at$X = 0$, $(\tau \geq 0)$ in addition to symmetry the shear stress about line $X = 0$ .also from these figures we note changing in the sign of the shear stress that not mean flow separation because the velocity of the wall is limited . Similarly Shear stress distribuation on the lower wall, in Fig. (5a) shear stress distribution increases with an increases curvature effects at $X = 0$ in addition to symmetry the shear stress about line $X = 0$ which does not happen in Fig. (5b) at increasing of Reynold's number .Also in Fig. (5c) shear stress distributions increases with an increases values of amplitude of the channel at $X = 0$, $(\tau \geq 0)$ in addition to symmetry the shear stress about line $X = 0$.From these figures we note changing in the sign of the shear stress

These results is agreement with the numerical results which obtained in [16], [21].

Pumping (pressure drop characteristics):-

In this section we study a distinctive characteristic of peristaltic motion for hybrid nano-fluid is pumping that is the relationship between Δp and $\bar{Q}$ which is summarized in Fig. (6) .we note that pressure rise (Δp) is a function of 3rd degree of time mean flow rate $(\bar{Q})$ as seen in (3.21) in addition to parameters Reynolds number(R_e), wave

number(δ), wave amplitude(a),solid volume fraction of nanoparticles of Al_2O_3 and Cu (ϕ_1, ϕ_2) ,base fluid density(ρ_f), the density of Al_2O_3 and Cu (ρ_{s_1} , ρ_{s_2}).

Fig. (6-a) shows The variation of pressure gradient Δp with time mean flow rate $\bar{Q}$ with given$\delta = 0.1$, $a = 0.2$, $\phi_1 = 0.1$ and $\phi_2 = 0.03$ for different values of Reynolds number($R_e = 0,100,200,400$) . We observed that at small value of Reynolds number$R_e = 0$, the graph (Δp - $\bar{Q}$)is straight line and this linearity completely disappears at the large values of Reynolds number like 200 or 400.Moreever at $\Delta p \geq 0$ and $\bar{Q} \geq 0$ for large Reynolds number ($R_e = 200,400$) there is no any pumping

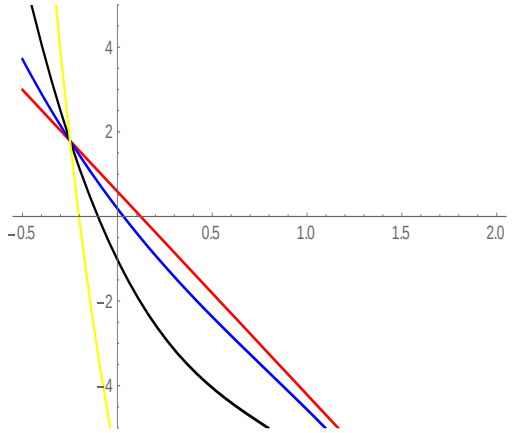

Fig. (6-a).The variation of pressure gradient Δp with time mean flow rate $\bar{Q}$

In peristaltic motion the pumping is always characterized by the relation between the time mean flow rate $\bar{Q}$ to the pressure difference Δp at the ends of the channel. With respect to the pressure

$$p = \sum_{n=0}^{\infty} \delta^n p_n \qquad (4.1)$$

From equations (2.5) & (2.6), we get p_0 , p_1 and p_2 with the same the previous technique in stream function and heat transfer

0th order (δ^0) :-

$$p_{0x} = \frac{1}{E_2}\psi_{0yyy}\,, \tag{4.2}$$

$$p_{0y} = 0\,.$$

1th order (δ^1) :-

$$p_{1x} = \frac{1}{E_2}\{\psi_{1yyy} - R_e E_1 E_2\left(\psi_{0y}\psi_{0yx} - \psi_{0x}\psi_{0yy}\right)\}\,, \tag{4.3}$$

$$p_{1y} = 0\,.$$

2nd order (δ^2) :-

$$p_{2x} = \frac{1}{E_2}\{\psi_{2yyy} + \psi_{0yxx}\} - R_e E_1\left(\psi_{0y}\psi_{1yx} + \psi_{1y}\psi_{0yx} - \psi_{0x}\psi_{1yy} - \psi_{1x}\psi_{0yy}\right), \tag{4.4}$$

$$p_{2y} = -\frac{1}{E_2}\psi_{0xyy}$$

We can calculate p_0 , p_1 and p_2 from expressions ψ_0 , ψ_1 and ψ_2 in the (x, y) coordinate by using the transformation which transform the domain of variable cross section a symmetric channel into a channel with straight walls

$$p_{0x} = -\frac{3q}{2E_2\eta^3} - \frac{3}{E_2\eta^2} \qquad p_{0y} = 0 \tag{4.5}$$

$$p_{1x} = E_1 R_e\{\frac{27q^2\eta'}{70\ \eta^3} + \frac{3q\eta'}{35\eta^2} - \frac{6\eta'}{35\,\eta}\} \qquad p_{1y} = 0 \tag{4.6}$$

$$p_{2y} = -\frac{9qy\eta'}{2E_2\eta^4} - \frac{6y\eta'}{E_2\eta^3}\,,$$

$$p_{2x} = -\frac{11\ {E_1}^2 E_2 {R_e}^2\ {\eta'}^2}{1225} + \frac{9q{y}^2{\eta'}^2}{E_2\eta^5} + \frac{9{y}^2{\eta'}^2}{E_2\eta^4} - \frac{21q{\eta'}^2}{10E_2\eta^3} + \frac{78\ {E_1}^2 E_2 {R_e}^2 q^3 {\eta'}^2}{13475\eta^3} - \frac{18{\eta'}^2}{5E_2\eta^2} + \frac{13\ {E_1}^2 E_2 {R_e}^2 q^2 {\eta'}^2}{13475\eta^2} - \frac{2\ {E_1}^2 E_2 {R_e}^2 q{\eta'}^2}{175\eta} - \frac{127\ {E_1}^2 E_2 {R_e}^2 q\eta''}{11550} - \frac{9q{y}^2\eta''}{4E_2\eta^4} - \frac{3{y}^2\eta''}{E_2\eta^3} + \frac{3q\eta''}{20E_2\eta^2} - \frac{117\ {E_1}^2 E_2 {R_e}^2 q^3\eta''}{26950\eta^2} + \frac{6\eta''}{5E_2\eta} - \frac{158\ {E_1}^2 E_2 {R_e}^2 q^2\eta''}{13475\eta} - \frac{166\ {E_1}^2 E_2 {R_e}^2 \eta\ \eta''}{40425}. \quad (4.7)$$

Where the prime ($'$) refers to the ordinary differentiation with respect to x. From these relations we have the pressure in x and y direction is a function of x, y up to second order (δ^2), also we note thate both p_{0y} and p_{1y} equal zero but p_{2y} not equal zero.

We define the difference of the pressures averaged over the cross section at axial stations $x = 0$ & $x = L$ (length of the channel) the mean pressure difference (Δp_L),

$$\Delta p_L = \frac{1}{2\eta_{x=0}} \int_{-\eta_{x=0}}^{\eta_{x=0}} p(0)dy - \frac{1}{2\eta_{x=L}} \int_{-\eta_{x=L}}^{\eta_{x=L}} p(L)dy. \quad (4.8)$$

We assume that L is an integral multiple of λ, so the pressure difference(Δp) over $\lambda = 1$ is

$$\Delta p = \frac{1}{\eta_{x=0}} \int_{-\eta_{x=0}}^{\eta_{x=0}} \left(\int_0^{\lambda} \frac{\partial p}{\partial x} dx\right) dy. \quad (4.9)$$

Where η is periodic with period λ . from equations (4.2), (4.3),(4.4),(4.5),(4.6),(4.7) and (4.9)

$$\Delta p = (\Delta p)_0 + \delta\ (\Delta p)_1 + \delta^2 (\Delta p)_2 + O(\delta^3).$$

Where :-

$$(\Delta p)_0 = \frac{1}{\eta_{x=0}} \int_{-\eta_{x=0}}^{\eta_{x=0}} \left(\int_0^{\lambda} p_{0x}\, dx\right) dy,$$

$$(\Delta p)_1 = \frac{1}{\eta_{x=0}} \int_{-\eta_{x=0}}^{\eta_{x=0}} \left(\int_0^{\lambda} p_{1x}\, dx\right) dy, \tag{4.10}$$

$$(\Delta p)_2 = \frac{1}{\eta_{x=0}} \int_{-\eta_{x=0}}^{\eta_{x=0}} \left(\int_0^{\lambda} p_{2x}\, dx\right) dy.$$

The different integrals appearing in (4.10) are given in appendix (2) which evaluated using the software package Mathematica 4.1and are presented in appendix (3) .in this paper we prescribe the peristaltic waves on the wall by

$$\eta = 1 + a\ \cos 2\pi x, \quad \text{Upper wall} \tag{4.11}$$

$$-\eta = -1 - a\ \cos 2\pi x \quad \text{Lower wall}$$

Where a is dimensionless amplitude of the wave. after calculating all the integrals we get the pressure rise over $\lambda = 1$ which is independent of y.

$$(\Delta p)_0 = \frac{-6}{E_2}\left\{\frac{1}{(1-a^2)^{\left(\frac{3}{2}\right)}} + \frac{(2+a^2)q}{4(1-a^2)^{\left(\frac{5}{2}\right)}}\right\},$$

$$(\Delta p)_1 = 0, \tag{4.12}$$

$$(\Delta p)_2 = \frac{-788}{40425}\pi^2 a^2\, E_2\, (R_e E_1)^2 - \frac{16}{175}\pi^2\, q\, E_2\, (R_e E_1)^2\left(1 - \sqrt{1-a^2}\right) - \frac{232}{2695}\pi^2 E_2\, q^2 (R_e E_1)^2\left(-1 + \frac{1}{\sqrt{1-a^2}}\right)$$

$$-\frac{156}{13475}\,\pi^2 a^2 q^3 E_2 (R_e E_1)^2 \frac{1}{(1-a^2)^{\left(\frac{3}{2}\right)}} - \frac{96}{5E_2}\pi^2\left(-1 + \frac{1}{\sqrt{1-a^2}}\right)$$

$$-\frac{36}{5E_2}\,\pi^2 a^2 q \frac{1}{(1-a^2)^{\left(\frac{3}{2}\right)}}\ .$$

We can write the pressure difference (Δp) as follow

$$\Delta p = \varphi_0 + \varphi_1 q + \varphi_2 q^2 + \varphi_3 q^3 + O(\delta^3).$$

Were

$$\varphi_0 = 2\{\frac{-3}{E_2(1-a^2)^{\left(\frac{3}{2}\right)}} - 0.009744\ \pi^2 a^2\delta^2 E_2(R_e E_1)^2 - \frac{48}{5E_2}\pi^2\delta^2\left(-1+\frac{1}{\sqrt{1-a^2}}\right)\},$$

$$\varphi_1 = 2\{\frac{-3(2+a^2)}{4E_2(1-a^2)^{\left(\frac{5}{2}\right)}} - \frac{18}{5E_2}\frac{\pi^2 a^2\delta^2}{(1-a^2)^{\left(\frac{3}{2}\right)}} - 0.045708\ \pi^2 E_2(R_e E_1)^2\delta^2\left(1-\sqrt{1-a^2}\right)\},$$

$$\varphi_2 = 2\{-0.043044\ \pi^2 E_2\ \delta^2(R_e E_1)^2\left(-1+\frac{1}{\sqrt{1-a^2}}\right)\},$$

$$\varphi_3 = 2\{-0.005792\,\pi^2 a^2\delta^2 E_2(R_e E_1)^2\frac{1}{(1-a^2)^{\left(\frac{3}{2}\right)}}\}.$$

We want to express the pressure difference in terms the mean flow rate $\bar{Q} = (q+2)$ up to the 2nd order of δ.we can write the pressure difference

$$\Delta p = \mathcal{E}_0 + \mathcal{E}_1\bar{Q} + \mathcal{E}_2\bar{Q}^2 + \mathcal{E}_3\bar{Q}^3, \qquad (3.21)$$

Were

$$\boldsymbol{\mathcal{E}_0 = \varphi_0 - 2\varphi_1 + 4\varphi_2 - 8\varphi_3,}$$
$$\boldsymbol{\mathcal{E}_1 = \varphi_1 - 4\varphi_2 + 12\varphi_3,}$$
$$\boldsymbol{\mathcal{E}_2 = \varphi_2 - 6\varphi_3,}$$
$$\boldsymbol{\mathcal{E}_3 = \varphi_3.}$$

We note that the coefficients $\boldsymbol{\varphi_0, \varphi_1, \varphi_2}$ and $\boldsymbol{\varphi_3}$ are functions of the non-dimensional parameters $\boldsymbol{\delta}$, $\boldsymbol{a}$ and $\boldsymbol{R_e}$. From the relations (4.12) we note that $\boldsymbol{(\Delta p)_1 = 0}$, then we find no term proportional with $\boldsymbol{R_e}$ .if we put $\boldsymbol{R_e = 0}$, $\boldsymbol{\delta \neq 0}$ we get streamline curvature effects. But if we put $\boldsymbol{\delta = 0}$, $\boldsymbol{R_e \neq 0}$ this case isn't possible.

Conclusions: -

In the present analysis, we examine the effects curvature, inertia force, nano particles volume fraction, and heat source/sink of an incompressible, viscous fluid of (Cu–) hybrid nanofluid with heat transfer in an asymmetric channel with supple walls by peristaltic transport, also the two shape factors of the nanofluid were considered (spherical and cylindrical nanoparticles). The effects of various physical parameters are considered on the axial and normal velocities, streamlines, heat distribution, shear stress on the walls, Nusselt number, normal force, and entropy generation. The main outcomes of this study are summarized as follows:

1. The physical properties of aluminum oxide nanoparticles improve the axial motion of (bio-fluid) blood, while the physical properties of copper nanoparticles improve the normal motion of (bio-fluid) blood, so the hybrid nanoparticles enhance the biological motion.
2. The temperature of the fluid for hybrid nanofluid (blood model) is less than that for the clear fluid. So, the hybrid nanofluid gives us control over the temperature of the patients.
3. The perturbation method solution obtained here, after we introduce the domain transformation, gives us improved accuracy for the discussion of several phenomena, such as pumping and trapping, and so on.
4. An increase in solid volume fraction, heating source, Reynolds, and Prandtl numbers increases the Nusselt number.
5. The fluid temperature increases for increasing values of wave amplitude, Reynolds, Prandtl numbers, and the heat source while decreases for increasing values of flow rate, sink heating, and solid volume fraction $\phi 1$ and $\phi 2$.

6. Shear stress of copper nanofluid is the highest due to the frictional force of copper is high.
7. When the generated shear stress distribution on the vessel's blood wall exceeds a certain maximum limit (this is according to damaged blood constituents). In this case, the magnitude of the shear stress distribution has an important role in the process of molecular convective.

REFERENCES

Das S, Jana RN, Makinde OD. MHD flow of (Cu-Al2O3)/water hybrid nanofluid in porous channel: analysis of entropy generation. Defect Diffus Forum. 2017;377:42-61. https://doi.org/10.4028/www.scientific.net/ddf.377.42

Chamkha AJ, Dogonchi AS, Ganji DD. Magneto-hydrodynamic flow and heat transfer of a hybrid nanofluid in a rotating system among two surfaces in the presence of thermal radiation and Joule heating. AIP Adv. 2019;9:025103. https://doi.org/10.1063/1.5086247

Usman M, Hamid M, Zubair T, Ul Haq R, Wang W. (Cu-Al2O3)/water hybrid nanofluid through a permeable surface in the presence of nonlinear radiation and variable thermal conductivity via LSM. Int J Heat Mass Transfer. 2018;126:1347-1356. https://doi.org/10.1016/j.ijheatmasstransfer.2018.06.005

Abdelsalam SI, Mekheimer KhS, Zaher AZ. Alterations in blood stream by electroosmotic forces of hybrid nanofluid through diseased artery:

aneurysmal/stenosed segment. Chinese J Phys. 2020;67:314-329. https:// doi.org/10.1016/j.cjph.2020.07.011

Sadaf H, Abdelsalam SI. Adverse effects of a hybrid nanofluid in a wavy non-uniform annulus with convective boundary conditions. RSC Adv. 2020;10:15035-15043. https://doi.org/10.1039/D0RA01134G.

Abo-Elkhair RE, Bhatti MM, Mekheimer KhS. Magnetic force effects on peristaltic transport of hybrid bio- nanofluid (AuCu nanoparticles) with moderate Reynolds number: an expanding horizon. Int Commun Heat Mass Transfer. 2021;123:105228. https://doi.org/10.1016/j.icheatmasstransfer.2021.105228

Saba F, Ahmed N, Khan U, Waheed A, Rafiq M, Mohyud-Din ST. Thermophysical analysis of water based (Cu-Al2O3) hybrid nanofluid in an asymmetric channel with dilating/squeezing walls considering different shapes of nanoparticles. Appl Sci. 2018;8:1549. https://doi.org/10.3390/app8091549.

Jahar S, Pradyumna G, Arjumand A. A review on hybrid nanofluids: recent research, development and applications. Renew Sustain Energy Rev. 2015;43:164-177. https://doi.org/10.1016/j.rser.2014.11.023.

Raza J, Rohni AM, Omar Z. Numerical investigation of copper-water (Cu-Water) nanofluid with different shapes of nanoparticles in a channel with stretching wall: slip effects. Math Comput Appl. 2016;21:43.

https://doi.org/10.3390/mca21040043

Ramzan M, Gul H, Chung JD, et al. Significance of Hall effect and Ion slip in a three-dimensional bioconvective Tangent hyperbolic nanofluid flow subject to Arrhenius activation energy. Sci Rep. 2020;10: 18342. https://doi.org/10.1038/s41598-020-73365-w

Nagarajan N, Akbar S. Heat transfer enhancement of Cu-water nanofluid in a porous square enclosure driven by an incessantly moving flat plate. Proc Eng. 2015;21:279-286. https://doi.org/10.1016/j.proeng. 2015.11.369

Maruthi PK, Subadra N, Srinivas MAS. Study of peristaltic motion of nano particles of a micropolar fluid with heat and mass transfer effect in an inclined tube. Procedia Eng. 2015;127: 694-702. https://doi.org/10. 1016/j.proeng.2015.11.368

Liaquat AL, Zurni O, Ilyas K, Asiful HS, El-Sayed MS, Nisar KS. Stability analysis and multiple solution of CuAl2O3/H2O nanofluid contains hybrid nanomaterials over a shrinking surface in the presence of viscous dissipation. J Mater Res Technol. 2020;9:421-432. https://doi.org/10.1016/j.jmrt.2019.10.071

Bejan A. The method of entropy generation minimization. In Energy and the Environment, Part of the Environmental Science and Technology Library book series (ENST, volume 15), Springer, The Netherlands. 1999:11-22. https://doi.org/10.1007/978-94-011-4593-0_2

Mahmud S, Fraser RA. Thermodynamic analysis of flow and heat transfer inside channel with two parallel plates. Exergy, Int J. 2002;2:140-146. https://doi.org/10.1016/S1164-0235(02)00062-6

Mahmud S, Fraser RA. The second law analysis in fundamental convective heat transfer problems. Int J Thermal Sci. 2002;42:177-186. https://doi.org/10.1016/S1290-0729(02)00017-0

Rashidi MM, Nasiri M, Shadloo MS, Yang Z. Entropy generation in a circular tube heat exchanger using nanofluids: effects of different modeling approaches. Heat Transfer Eng. 2017;38:853-866. https://doi.org/ 10.1080/01457632.2016.1211916

Sohail M, Naz R, Abdelsalam SI. On the onset of entropy generation for a nanofluid with thermal radiation and gyrotactic microorganisms through 3D flows. Physica Scripta. 2020;95:045206. https://doi.org/10.1088/ 1402-4896/ab3c3f

Riaz A, Zeeshan A, Bhatti MM. Entropy analysis on a three-dimensional wavy flow of eyringpowell nanofluid: a comparative study. Math Prob Eng. 2021;2021:6672158. https://doi.org/10.1155/2021/6672158

Riaz A, Bhatti MM, Ellahi R, Zeeshan A, Sait MS. Mathematical analysis on an asymmetrical wavy motion of blood under the influence entropy generation with convective boundary conditions. Symmetry. 2021;12: 102. https://doi.org/10.3390/sym12010102

Zeeshan A, Shehzad N, Abbas T, Ellahi R. Effects of radiative electro-magnetohydrodynamics diminishing internal energy of pressure-driven flow of titanium dioxide-water nanofluid due to entropy generation. Entropy. 2019;21:236. https://doi.org/10.3390/e21030236

Jaffrin MY, Shapiro AH. Peristaltic pumping. Annual Rev Fluid Mech. 1971;3:13-37. https://doi.org/10. 1146/annurev.fl.03.010171.000305

Fung YC, Yih CS. Peristaltic transport. ASME J Appl Mech. 1968;35:669-675. https://doi.org/10.1115/1. 3601290

Yin F, Fung YC. Peristaltic waves in circular cylindrical tubes. ASME J Appl Mech. 1969;36:579-587. https:// doi.org/10.1115/1.3564720

Rath HJ. Peristaltische Stromungen. Berlin: Springer; 1980.

Shapiro A, Jaffrin M, Weinberg S. Peristaltic pumping with long wavelengths at low Reynolds number. J Fluid Mech. 1969;37:799-825. https://doi.org/10.1017/S0022112069000899

Selverov KP, Stone HA. Peristaltically driven channel flows with applications toward micromixing. Phys Fluids. 2001;13:1837-1859. https://doi.org/10.1063/1.1377616

Yi M, Bau HH, Hu H. Peristaltically induced motion in a closed cavity with two vibrating walls. Phys Fluids. 2002;14:184-197. https://doi.org/10.1063/1.1425841

Jaffrin MY. Inertia and streamline curvature effects on peristaltic pumping. Int J Eng Sci. 1973;11:681-699. https://doi.org/10.1016/0020-7225(73)90029-3

Abdelsalam SI, Sohail N. Numerical approach of variable thermophysical features of dissipated viscous nanofluid comprising gyrotactic micro-organisms. Pramana—J Phys. 2020;94:67. https://doi.org/10.1007/ s12043-020-1933-x

Abumandour RM, Eldesoky IM, Kamel MH, Ahmed MM, Abdelsalam SI. Peristaltic thrusting of a thermal- viscosity nanofluid through a resilient vertical pipe. Zeitschrift fr Naturforschung A. 2020;75:727-738.

https://doi.org/10.1515/zna-2020-0054

Abdelsalam SI, Bhatti MM. Anomalous reactivity of thermo-bioconvective nanofluid towards oxytactic microorganisms. Appl Math Mech-Engl Ed. 2020;41:711-724. https://doi.org/10.1007/s10483-020-2609-6

Mekheimer KhS, Hasona WM, Abo-Elkhair RE, Zaher AZ. Peristaltic blood flow with gold nanoparticles as a third grade nanofluid in catheter: application of cancer therapy. Phys Lett A. 2018;382:85-93. https://doi. org/10.1016/j.physleta.2017.10.042

Mekheimer KhS, Abo-Elkhair RE, Moawad AMA. Electrothermal transport via gold nanoparticles at antimicrobial of blood flow through an electro-osmosis artery with overlapping stenosis. Int J Fluid Mech Res.

2020;47:135-152. https://doi.org/10.1615/InterJFluidMechRes.2020026831

Abo-Elkhair RE, Mekheimer KhS, Zaher AZ. Electro-magnetohydrodynamic oscillatory flow of a dielectric fluid through a porous medium with heat transfer: Brinkman model. BioNanoSci. 2018;8:596-608. https://doi.org/10.1007/s12668-018-0515-6

Mekheimer KhS, Abo-Elkhair RE, Moawad AMA. Electro-osmotic flow of non-newtonian biofluids through wavy micro-concentric tubes. BioNanoSci. 2018;8:723-734. https://doi.org/10.1007/s12668-018- 0523-6

Manton M. Long-wavelength peristaltic pumping at low Reynolds number. J Fluid Mech. 1975;68:467-476. https://doi.org/10.1017/S0022112075001760

Souidi F, Ayachi K, Benyahia N. Entropy generation rate for a peristaltic pump. J Non-Equilibrium Thermodyn. 2009;34:171-194. https://doi.org/10.1515/JNETDY.2009.010

Woods LC. Thermodynamics of Fluid Systems. Oxford: Oxford University Press; 1975.

Rao AR, Mishra M. Nonlinear and curvature effects on peristaltic flow of a viscous fluid in an asymmetric channel. Acta Mech. 2004;168:35-59. https://doi.org/10.1007/s00707-004-0079-0.